Biophysical Chemistry, 30 (1988) 225–236
Elsevier

BPC 01259

Phosphorescence of adenosine and poly(riboadenylic acid)

Evidence for dual emissions and $n\pi^*$ states

M. Daniels [a], J.-P. Ballini [b], A. Gräslund [c], A. Rupprecht [d] and L. Åsbrink [e]

[a] *Chemistry Department, Oregon State University, Corvallis, OR 97331, U.S.A.,*
[b] *Laboratoire de Physique et Chimie Biomoleculaire, Institut Curie, Université Paris VI, Paris, France,*
[c] *Department of Biophysics and*
[d] *Department of Physical Chemistry, Arrhenius Laboratory, University of Stockholm, S-106 91 Stockholm and*
[e] *Physics Department, Royal Institute of Technology, S-100 44 Stockholm, Sweden*

Received 28 October 1987
Revised manuscript received 2 February 1988
Accepted 26 February 1988

Phosphorescence; Adenosine; Poly(riboadenylic acid)

Phosphorescence from the 9-adenylyl group in the form of microcrystalline powders of adenosine films of poly(riboadenylic acid) (poly(rA)) in hyaluronic acid has been studied at 77 K. For adenosine, clearly resolved vibronic structure consists of two progressions, A and B, with $\Delta\bar{\nu}_A = 1363$ cm^{-1} and $\Delta\bar{\nu}_B = 1575$ cm^{-1}, correlated with in-plane C_5-N_7 and in-plane C_4-C_5 stretch, respectively. The relative strength of the progressions varies with excitation wavelength and this, together with the absence of a common origin, indicates the existence of two independent emitting states with 0-0′ levels separated by either 300 or 1000 cm^{-1}. Two different excitation spectra are observed lying below the normal ($\pi\pi^*$) adsorption and one is assigned as a previously undetected $^1(n\pi^*)$ transition. For poly(rA) films the emission band envelope is identical with that of adenosine but the vibronic structure is lost. Only one excitation peak is observed at 32.9×10^3 cm^{-1}, identical with one of the adenosine spectra. The second adenosine excitation spectrum probably represents an intermolecular charge transfer transition. Comparison is made with the predictions of six semi-empirical MO calculations.

1. Introduction

Despite continuing efforts over the past 30 years there is still considerable uncertainty concerning the lower electronic transitions and excited states of 9-substituted adenines. Early studies of solvent and substituent effects [1] allowed the inference that there were two in-plane (π, π^*) transitions in the first absorption band with the lowest energy transition polarized along the long axis, and a variety of subsequent experimental work has been directed to determining the intensities, locations and polarizations of these transitions, with somewhat discordant results. Polarized absorption spectroscopy of single crystals of 9-methyladenine [2,3] showed a strong transition (oscillator strength 0.28) at 275 nm, essentially along the polarized short axis. A second transition at 255 nm was much weaker (oscillator strength 8×10^{-3}), in-plane polarized and perpendicular to the first transition. Linear dichroism measurements of dispersions of solutes oriented in stretched films avoid possible problems due to crystal interactions, and such measurements on 9-methyladenine in polyvinyl alcohol [4] provide clear evidence for a new transition at 286 nm in the low-energy tail of the absorption. Although adenosine did not show this effect, similar work on 6-(methylamino)-9-methylpurine [5] showed an enhanced and partially resolved absorption be-

Correspondence address: M. Daniels, c/o P. Vigny, Laboratoire de Physique et Chimie Biomoleculaire, 11 rue Pierre et Marie Curie, 75231 Paris Cedex 05, France.

tween 320 and 290 nm. It is perhaps significant that the first resolved vibronic band in the low-temperature fluorescence of AMP lies at 286 nm and can probably be assigned as the 0-0′ transition.

CD spectra of adenine nucleosides have been correlated with ultraviolet absorption by two different procedures, leading to contrasting conclusions. Assuming Gaussian profiles for the overall transition envelopes, Ingwall [6] found that transitions centered at 270, 260 and 250 nm (all within the 260 nm band envelope) could account for the ultraviolet and CD, as well as MCD spectra. The 260 and 250 nm transitions were assigned as $\pi \rightarrow \pi^*$, while the 270 nm transition was suggested to be n-π^* on the basis of its low absorption intensity, solvent red shift, solvent sensitivity of rotational strength, and strong blue shift on protonation. On the other hand, assuming a harmonic progression of Gaussian vibronic bands, Fornasiero et al. [7] have fitted the CD and ultraviolet data for adenosine and AMP from 290 to 247 nm using only two transitions considered to be ($\pi\pi^*$) with (0-0′) levels at 269 nm (oscillator strength $\simeq 0.3$) and 275 nm (oscillator strength not given but presumably $< 10^{-2}$).

Other evidence on the location of electronic transitions comes from excitation profiles for preresonance and resonance Raman scattering in which enhancing transitions have been located at 276 and 260 nm [8], 276 and 269 nm [9], and 268.3 and 264.6 nm [10].

Unsatisfactory as the situation is for $\pi\pi^*$ transitions, it is even worse for ($n\pi^*$) transitions, not least on account of the paucity of experimental evidence. Stewart and Davidson [2] observed an out-of-plane absorption in co-crystals of 9-methyladenine and 1-methylthymine, with an onset at 300 nm and increasing continuously to 230 nm, and suggested that it may be an adenine $n \rightarrow \pi^*$ transition although it was not observed in pure crystals of 9-methyladenine. It has been suggested that CD [6,11,12] and MCD [13] spectra show evidence of participation of the $n\pi^*$ transition but no concrete conclusions have emerged from this work. Transmission methods, whether based on isotropic, or linearly or circularly polarized transitions, are inherently unsuitable for detecting very weak transitions such as $^1(n\pi^*)$ for which oscillator strengths of approx. 10^{-3} are anticipated. On the other hand, intersystem crossing is facilitated from $^1(n\pi^*)$ states, leading to enhanced phosphorescence emission [14] which can then be detected with high sensitivity. Indeed, phosphorescence excitation spectroscopy has been used to advantage in studying the $^1(n\pi^*)$ transition of purine, the parent molecule of adenines [15,16]. Accordingly, one of the aims of this work was to search for $^1(n\pi^*)$ transitions by phosphorescence detection. This prompted us to re-examine the phosphorescence emission spectra of adenosine and has led to the conclusion that there are two emitting states contributing to the phosphorescence band envelope, rather than the one which has been previously assumed. We show that this increases the understanding of results obtained in earlier studies.

We have investigated the phosphorescence of the 9-adenylyl group in two forms which have not been studied previously. First, adenosine has been investigated in the form of microcrystalline powders. Here the crystal structure [19] shows that the planes containing the adenine group are arranged so that there is stacking [20] of the N^6-amino group of the adenines in one plane over the midpoint of the C_4–C_5 bond of the adenine of the adjacent plane. Second, poly(rA) has been prepared by a fiber-extrusion process, as a dilute solid solution in a film of hyaluronic acid. Stacking interactions are possible within each poly(rA) strand but general crystal interaction effects may be discounted. Although the strands of poly(rA) are stretched by the process of fiber extrusion, the structure is probably much less ordered than that of the adenosine crystals. Studying these samples by phosphorescence spectroscopy has allowed us to characterize a previously undetected $^1(n\pi^*)$ transition of the adenine chromophore lying at a lower energy level than $(\pi\pi)^*$ transitions.

2. Experimental

The emission and excitation spectra were obtained using a modified Baird-Atomic model SF-100 spectrofluorimeter. Radiation from a magnetically stabilized 150 W xenon lamp was dispersed

by a double-grating monochromator and focussed on the sample capillary (1.5 mm, i.e., 'Spectrosil') in a standard (Baird-Atomic accessory) fused silica dewar having an elongated (8 cm) cylindrical, non-aluminized tail. The sample capillary was completely surrounded by liquid nitrogen so the sample may be reasonably assumed to be at 77 K. Emission from the sample was observed at right angles to the excitation beam and focussed through the second double-grating monochromator. Detection was by an EMI 6256 S photomultiplier cooled with pulverized solid CO_2 and operated in the photon-counting mode followed by an Ortec 9301 shaping pre-amplifier, 9302 linear amplifier and 436 discriminator. Counts were collected in a Nicolet 1072 instrument computer triggered by a pulse generated from the voltage ramp of the wavelength drive of the SF-100 spectrofluorimeter. Data were collected at a dwell time of 1 s/channel and the spectra were scanned at 1 nm/s. Signals were sufficiently intense that the narrowest slits (0.3 mm, giving a spectral slit width of 1.5 nm) were used on both excitation and emission, signal accumulation by multiple scanning being used only to verify weak features without losing resolution. Typical counting conditions were: photomultiplier dark count rate, 2–3 s^{-1}; background count rate, $\sim 10^2$ s^{-1}; count rate of adenosine, $\sim 3 \times 10^3$ s^{-1} at 402 nm and in excess of 2×10^4 s^{-1} at λ_{max}, depending on the excitation wavelength. The chopping speed was usually 4000 rpm and no bleaching was observed, either short-term or long-term. Background was measured first with an empty capillary and then with nonluminescent $CaCO_3$ powder in place of the sample. Results were practically identical and without structure, indicating that the background is largely due to front-surface scatter from the dewar. This background was subtracted in the Nicolet instrument but all subsequent data treatment was carried out with an HP 9125 computer and 9862 plotter. All spectra presented here are corrected and normalized to facilitate comparison of band profiles; the emission spectra have been corrected for monochromator transmission efficiency and photomultiplier wavelength sensitivity relative to a standard tungsten lamp (Electro-Optics L-101) whose calibration is 'traceable to an NBS standard'; the excitation spectra have been corrected for variation in the wavelength of the output of the xenon lamp/excitation monochromator combination using as a 'quantum counter' a solution of rhodamine B in ethylene glycol (8 g/l) in a triangular cuvette.

The major effect of the corrections on the emission spectra is to strengthen the features at wavelengths beyond 550 nm by compensating for the fall-off in photomultiplier sensitivity in this range, while for excitation spectra the corrections compensate for the continuous fall-off in ultraviolet intensity with decreasing wavelength.

Samples, microcrystalline adenosine (Sigma) or a spun film of poly(rA), were placed in a Spectrosil capillary tube (2 mm inner diameter, 25 mm length) mounted on the end of a Teflon rod and adjusted in the horizontal plane so that excitation and emission beam axes were tangential to the surface. When using a film sample, the rod was rotated to optimize the signal and this occurred when the film was approx. 45° to the excitation and emission axes. The poly(rA)/hyaluronic acid film was prepared according to a wet spinning method [21a–c] using a spinning solution of 6.3 mg/ml of poly(rA) (Sigma) and 2.2 mg/ml of hyaluronic acid (Sigma) in 0.1 M KCl. 80% ethanol containing 0.1 M KCl was used as spinning bath. After the wet spinning, KCl was removed by bathing the cylinder with the spun deposit in 80% ethanol. The film was weakly birefringent but an X-ray diffraction pattern showed only diffuse rings.

Calculations of the transition energies and oscillator strengths have been carried out using the HAM/3 semi-empirical MO procedure [22] for 9-H-adenine in the Spencer geometry [23]. Repulsion integrals were calculated using the Mataga-Nishimoto expression and 30 configuration interactions were evaluated. Details of the parameterization are given in ref. 22.

3. Results

3.1. Emission spectra of adenosine

The phosphorescence spectra of adenosine at 77 K are presented in fig. 1. There are clearly

resolved bands between 400 and 480 nm followed by a region of heavy overlap to approx. 600 nm. Changing the excitation wavelength causes systematic variations in the intensities of the resolved bands without changing their positions. Thus, the 403 nm band diminishes considerably on going from 299 to 317 nm and has almost disappeared at 333 nm. The bands at 426 and 451 nm move in parallel with that at 403 nm. On the other hand, the bands at 416 and 444 nm increase in importance from 299 to 333 nm excitation. The effective resolution which we observe is demonstrated by the behavior of the peaks at 444 and 451 nm which have not been resolved in previous lower resolution work on dilute glasses. The spectra in fig. 1a–c appear to be largely composed of two subcomponent spectra. Based on the characteristics of the resolved bands a partial vibronic analysis into two progressions has been carried out, with the results indicated in table 1. The two vibronic progressions which we observe, 1363 and 1575 cm^{-1}, correspond to strong Raman transitions at 1340 and 1580 cm^{-1} [31] which are understood to be due to vibrations in which the C_5-N_7 stretching mode is predominant for the 1340 cm^{-1} vibration and the C_4-C_5 in-plane stretch in the case of the 1580 cm^{-1} vibration [8,32].

3.2. Excitation spectra for adenosine

The variation of emission spectra with excitation wavelength and the classification into two emission series have led us to investigate the excitation spectra of the series. Excitation spectra (fig. 2a–d) have been measured at the wavelengths of the major resolved emission peaks. Under our conditions of relatively low resolution, band overlap occurs in emission, increasing across the spectrum with increasing wavelength. Consequently, the excitation spectra represent, to varying extents, the overlapping emissions. The excitation spectrum for the 403 nm band of the A series consists of a single peak at 304 nm (fig. 2a). The excitation profile for 416 nm emission (B series) is quite different (fig. 2b) with a maximum at 331 nm and showing vibronic structue at 316 nm; however, the weak shoulder between 290 and 310 nm can be attributed to admixture of some A

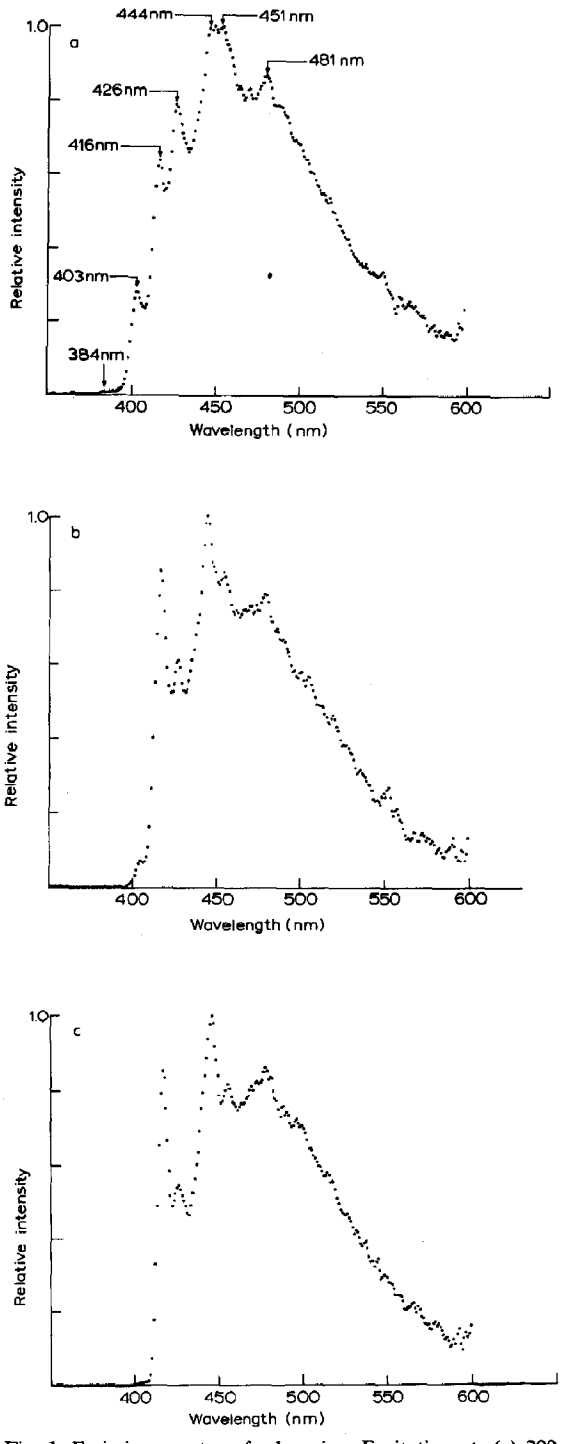

Fig. 1. Emission spectra of adenosine. Excitation at: (a) 299, (b) 317, (c) 330 nm

Table 1

Partial vibronic analysis of adenosine phosphorescence

Series A		Series B	
363 nm very weak		367 nm very weak	
381 nm weak		390 nm weak	
403 nm		416 nm	
426 nm	1355 cm^{-1}	444 nm	1566 cm^{-1}
451 nm	1351 cm^{-1}	478 nm	1580 cm^{-1}
481 nm	1384 cm^{-1}	517 nm	1580 cm^{-1}
514 nm			
$\Delta\bar{\nu} = 1363\ cm^{-1}$		$\Delta\bar{\nu} = 1575\ cm^{-1}$	

series character. At 426 nm, a member of the A series progression, the profile (fig. 2c) clearly resembles an overlap of the 403 and 416 nm profiles roughly in the proportion 3 : 2. This admixture of character, which we attribute to overlapping of the emission bands, persists at 447 nm (fig. 2d) which lies between the emission peaks at 444 and 451 nm, and also at 480 nm. We conclude that the excitation studies show the presence of two basis spectra correlating respectively with the A and B series emissions. The excitation vibrational splitting corresponding to the B series is 1360 cm^{-1}.

The phosphorescence of adenosine and related compounds such as 9-methyladenine, deoxyadenosine and AMP has been reported in several papers [24–30] concerning dilute rigid glasses. Series of bands of alternating intensity have been pointed out [28] and this feature of the intensity has been used to separate the overall spectrum into two progressions, one 'strong' and one 'weak', corresponding in position to our A and B series

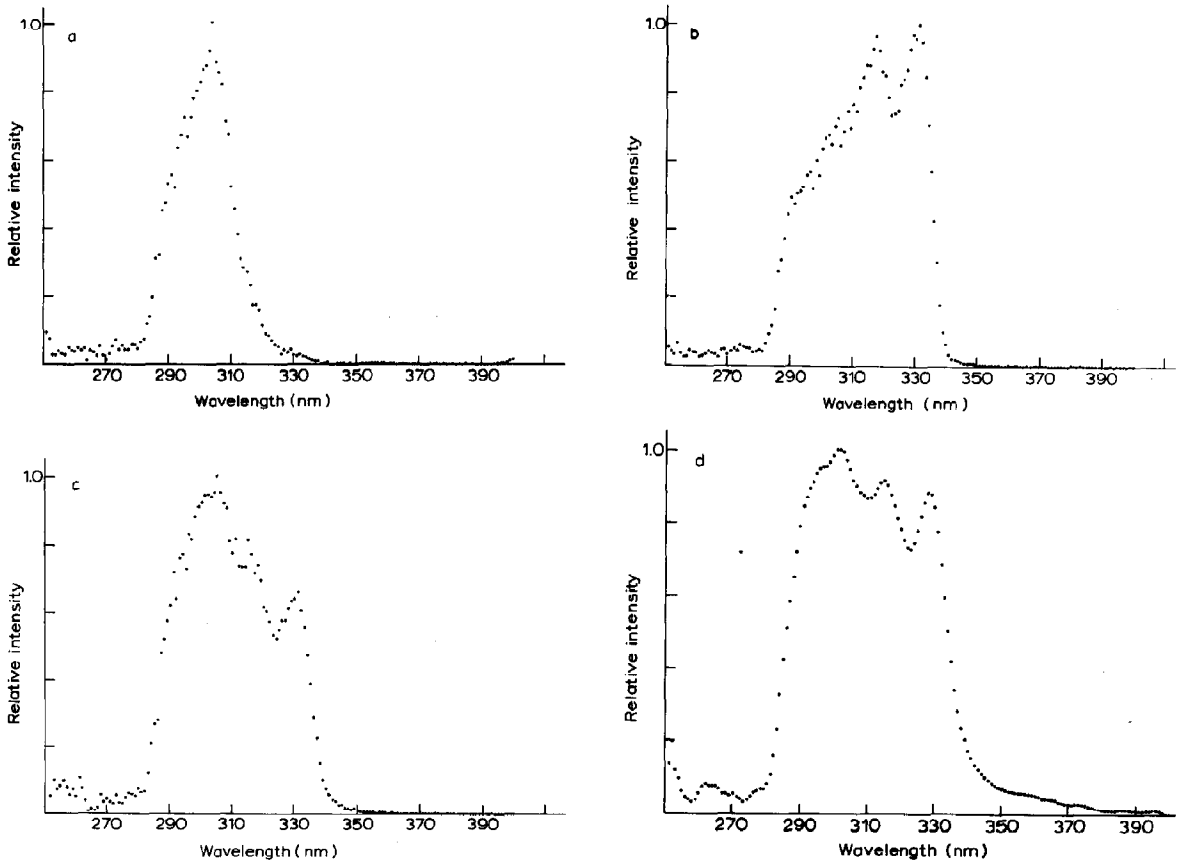

Fig. 2. Excitation spectra of adenosine. Monitored at: (a) 403, (b) 416, (c) 426, (d) 447 nm.

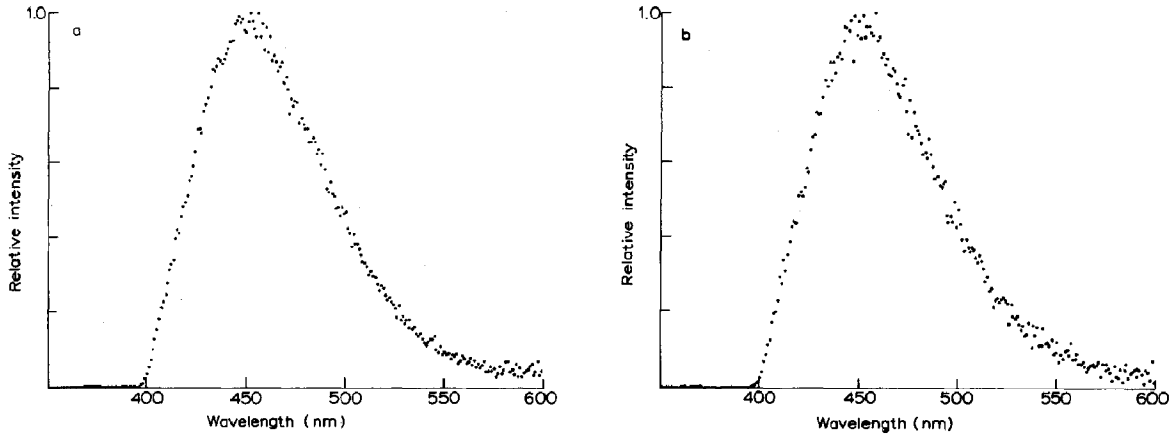

Fig. 3. Emission spectra of poly(rA)/hyaluronic acid film. Excitation at (a) 300, (b) 270 nm.

(note that, depending on excitation wavelength, we find that the B series can be strong). Some disagreements in earlier reports of band location, pointed out by Szerenyi and Dearman [27], can be rationalized on the basis of the solvent sensitivity of series B along the lines suggested by Kleinwächter et al. [28]. With this proviso we find no bands which have not been observed in dilute glass systems and in particular our results are in good agreement with those in refs. 25, 26 and 30. A characteristic feature in glasses is that the Franck-Condon profile peaks at the lower wavelength bands; the most intense band is usually at 402 nm and clearly resolved bands are seen at approx. 380 and approx. 390 nm, whereas we find the most intense bands at approx. 450 nm. This has led us to examine carefully the low-wavelength region with multiple scanning (10 times) and digital signal accumulation. We find evidence of weak emission below 400 nm and traces of very weak emission below 375 nm and these have been indicated in table 1 by extension of the series to higher energies. Note that the lowest emission band to be reported is at 366 nm for deoxy-AMP in diethyl ether/isopentane/ethanol (EPA) [27].

3.3. Emission spectra of poly(rA)

In overall profile, the phosphorescence of poly(rA) excited just outside the absorption band at 300 nm (fig. 3a) is very similar to that of adenosine (fig. 1a), peaking at approx. 450 nm and

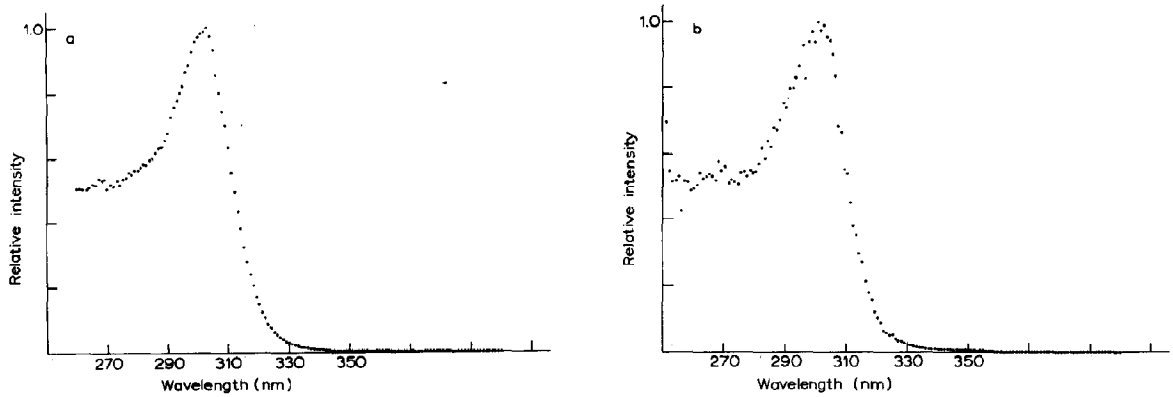

Fig. 4. Excitation spectra of poly(rA)/hyaluronic acid film. Monitored at: (a) 415, (b) 442 nm.

showing very little emission below 400 nm. A control sample of pure, wet-spun hyaluronic acid film gave only negligible phosphorescence under similar conditions. The most striking difference is the almost complete loss of resolved vibronic structure in poly(rA). This emission spectrum is identical with that obtained on excitation at 270 nm (fig. 3b), well within the $\pi\pi^*$ absorption band. Excitation at 343 nm causes a significant red shift with the peak moving to approx. 490 nm with a shoulder (~ 440 nm) which probably reflects a contribution of the 300 nm excitation spectrum. This red-shifted spectrum will be the subject of a separate communication.

3.4. Excitation spectra of poly(rA)

The excitation spectra monitored at 415 and 443 nm are strikingly similar to each other (fig. 4a and b) and to the profile for adenosine which we assign to the A series vibronic spectra (fig. 2a). The principal differences between the poly(rA) and adenosine spectra are the order of magnitude increase in efficiency as compared with adenosine in the case of excitation in the $\pi\pi^*$ band (260–280 nm) in poly(rA) and the absence of an excitation spectrum corresponding to transition B of adenosine (fig. 2b–d).

Discussion

4.1. Assignment and nature of emission spectra

It is clear from both our results on adenosine and literature results for glasses [28,29] that there are two major vibronic progressions in the phosphorescence spectra of 9-substituted adenines. However, consideration of other evidence strongly suggests that both of these progressions arise from distinct electronic states. If the progressions were to emanate from the same state then they would have a common origin which can be located by extrapolation of each series. Effective coincidence within the limits of resolution in our experiments can occur if $E(0\text{-}0)$ is at 346 nm for the A series and at 347 nm for the B series. Multiple scanning failed to reveal any emission below 360 nm. However, this cannot be taken to be definitive in our work because the emission is strongly forbidden at the origin. In glasses where the lower members of the progressions are enhanced, a similar search by Cohen and Goodman [30] around 28.5×10^3 cm^{-1} (350 nm) also proved fruitless. Thus, the source from which the emission stems may be located in either 380–390 or 360–370 nm region. The observation of a peak at 366 nm for deoxy AMP in EPA [27] suggests the latter region for one of the series but further investigation of this point is necessary. Further support for the independent dual emission is provided by consideration of the excitation spectra. Essentially, each progression has a distinct excitation spectrum, the main characteristics of which are demonstrated in fig. 2a and b. Lastly, we note the observation of the biexponential decay of AMP in ethylene glycol glass at 77 K, measured by averaging 16 decays over three decades [33].

Evidence concerning the nature of the emissions comes first from a consideration of polarization studies [29,30] of glasses. Both groups find that the polarization of the strong peaks (in an alternating sequence) is strongly negative with respect to excitation at 280 nm [30] and 290 nm (V. Kleinwächter, personal communication). However, between the strong peaks the polarization decreases (becomes less negative) to extrema at wavelengths corresponding to the 'alternate' (weaker) vibronic sequence. This oscillating pattern of behavior of polarization is presented clearly in the paper of Drobnik et al. [29], however, inspection shows that it also exists in the results obtained by Cohen and Goodman [30]. These polarization extrema correlate directly with the vibronic series A and B. Thus, series A, based on the in-plane C_4-C_5 stretch, has a degree of polarization of -0.20 while series B, due to the C_5-N_7 in-plane stretch, has a degree of polarization of approx. -0.05 (these values may not be accurate because of band overlap, but this is not important for the present discussion). Essentially, the series A transition is approximately perpendicular to the absorption transition at 280–290 nm, and series B is approx. 40° to this absorption, both emissions being polarized in-plane. Since $^3(\pi\pi)^*$ transitions are polarized out-of-plane [34] while those of the

$^3(n\pi)^*$ type are polarized in-plane [35] the adenosine phosphorescences are substantially of the $^3(n\pi)^*$ form. Although this stands in contradiction to the conclusions drawn by the previous workers, it should be noted that vibrational assignments were not available at that time and that neither group discussed the oscillatory behavior of the emission polarization. The major argument presented at that time in favor of $^3(\pi\pi)^*$ as the assignment was based on phosphorescence polarization excitation spectra. The polarization (of the main emission peak) was measured as a function of excitation wavelength across the absorption band and appeared to be invariant with respect to the wavelength. As the absorption band was presumed to encompass two mutually perpendicular in-plane $\pi\pi^*$ transitions (see section 1), it was concluded that the emission could only be polarized out-of-plane. However, close scrutiny of the results reveals that despite the 8 nm bandwidth of the exciting radiation, the polarization actually oscillates with respect to the excitation wavelength and the result is better understood with the aid of a model of two absorption and two emission transitions in which all transitions are in-plane. This point is being investigated further and will be the subject of a future communication.

4.2. *Assignment and nature of excitation spectra*

For adenosine we observe two independent excitation spectra which populate the different emission series and which we label correspondingly. Both excitation spectra lie outside the normal absorption spectrum, which probably corresponds to $^1(\pi\pi^*)$ transitions, and obviously populate the triplet manifold with high efficiency.

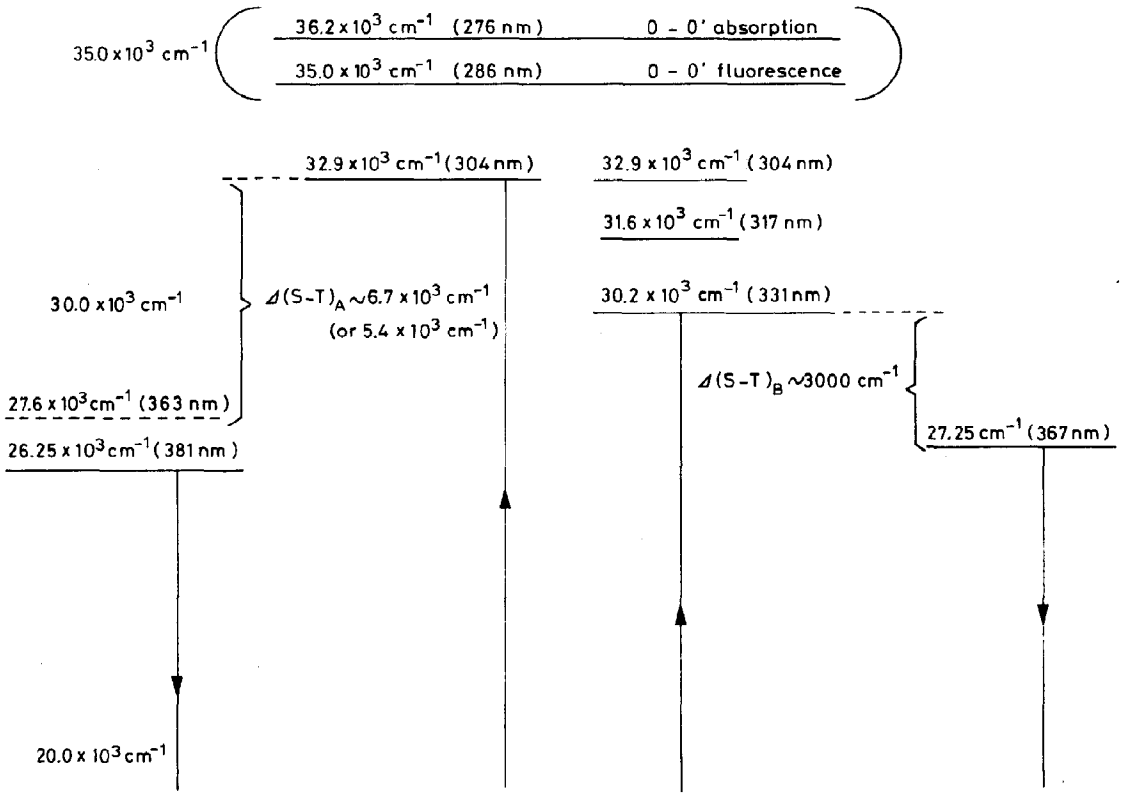

Fig. 5. Transition energies of adenosine.

Furthermore, there is no overlap with the emission spectra and we accordingly assign these spectra as singlet $n \rightarrow \pi^*$ transitions. The lowest energy transition, $^1(n\pi^*)_B$, has a clear vibrational structure and a strong 0-0′ band at 30.2×10^3 cm^{-1}. The origin of the $^1(n\pi^*)_A$ transition is not so clearly determined; the band is asymmetric and the maximum lies at 304 nm (32.9×10^3 cm^{-1}) as does the poly(rA) excitation spectrum (which has no overlap with higher vibrational levels of $^1(n\pi^*)_B$). The band maximum may well be the 0-0′ level; this is assumed in estimating singlet-triplet (S-T) and n_B-n_A splittings, and is represented in fig. 5.

The singlet-triplet splitting for the B series is 3.0×10^3 cm^{-1}, adopting the 0-0′ triplet level given by Szerenzi and Dearman [27] and this is quite consistent with the assignment of a pure $(n\pi^*)$ transition to absorbing and emitting B states (the absorption peak-to-emission peak value of 13700 cm^{-1} reported by Cohen and Goodman [30] and used to support their assignment as $^3(\pi\pi)^*$ is clearly an overestimate). For the A series the S-T splitting is either 5.4×10^3 or 6.7×10^3 cm^{-1}, depending on the choice of 0-0′ level (381 or 363 nm), and is significantly greater than that for the B series. This may indicate a degree of $\pi\pi^*$ character mixed in with that of $n\pi^*$ due to the adjacent $\pi\pi^*$ level at 36.0×10^3 cm^{-1} [7–9]. In any case, it is comparable to the $^3(n\pi^*)$ splitting in pyrimidine (5.7×10^3 cm^{-1}) [17]. Polarization measurements should be informative in this respect but we have not been able to observe significant polarization in our present experiments. Lifetimes are also strongly nonexponential (M. Daniels and C.E. Fairchild, unpublished results) and this together with the lack of polarization is probably indicative of extensive energy transfer.

4.3. Poly(rA)

In overall profile the emission spectrum of the poly(rA)/hyaluronic acid film is very similar to that of the adenosine microcrystals, with the loss of vibronic resolution most probably due to site broadening. This lack of resolution does not allow us to distinguish between the A and B series in emission, however, the excitation spectrum clearly indicates the strength of the $^1(n\pi^*)_A$ transition and the virtual absence of that of the $^1(n\pi^*)_B$ type found in adenosine.

Differences in behavior between the monomer and polymer have also been reported in studies in hydroxylic glasses. For these, AMP and adenosine give rise to a mixture of A and B emissions with the former type being the most intense [26–30], while poly(rA) gives either series B only, or a mixture of both, the B series being the most intense [27,33,36,37]. Absorption spectra of AMP and of poly(rA) are shifted under these conditions [38]; as a consequence, at a fixed excitation wavelength, different transitions may be excited in AMP and poly(rA). Hypochromism and/or hyperchromism, consequent to the stacking of poly(rA), may also be involved; more detailed investigations are clearly required. Whatever the explanation of the behavior in hydroxylic glasses, the reverse effect would seem to be operative in the poly(rA) film, i.e., if the structure of poly(rA)/glass leads to B-type emission, then the structure of poly(rA) film must differ significantly so as to lead to A-type behavior. Adequate structural information is lacking for both glass and film environments.

4.4. Comparison with purine and MO calculations

Purine, the parent molecule of adenine, is the only closely related molecule for which similar experimental data are available and it is appropriate to compare the experimental results for these two molecules. Difficulties in determining experimentally the characteristics of the lower excited states of adenine have led to a number of attempts to calculate their salient features. Indeed, this area is one of the rare examples of theoretical predictions predating experimental observation, unfortunately with results that are inconsistent in many cases, or even qualitatively incorrect.

The phosphorescence emission spectrum of purine was extensively investigated in various glasses at 77 K by Drobnik and Augenstein [39] who drew attention to the 'alternating intensity' behavior and the oscillating behaviour of polarization [29] without discussing the spectral origin or

interpeak polarizations. The first resolved emission band lies at 367 nm in EG and at 357 nm in EPA or isopropanol. However, for 9-ribosylpurine and 9-methyladenine, this band is missing and the first band lies at 383 and 385 nm, respectively (in isopropanol). The same behavior was observed by Cohen and Goodman [30] who describe the first purine band as appearing at 363 nm and the first band of 9-butyladenine at 378 nm, almost coincident with the second band of purine (all in EPA). This behavior introduces uncertainty into the determination of the 0-0′ level as discussed above for adenines, since the absence of the band may be due either to substitutional weakening of one transition or to the existence of emission from a proportion existing as the N(7)-H tautomer. Matrix-isolation studies on purine [16] at 20 K show the same alternating character: the first band is observed at 380 nm but the spectrum is not down to baseline at 375 nm and the possibility of a higher energy band occurring cannot be ruled out. The ^3E(0-0′) of unsubstituted purine thus lies at either 26.0×10^3 or approx. 27.8×10^3 cm^{-1}.

The $^1(n\pi^*)$ absorption of purine has been clearly established in studies on polarization excitation spectroscopy in EPA at 77 K [30], direct absorption in crystals [40] at 4 K, polarized reflectance spectroscopy at 295 K [41] and phosphorescence excitation spectroscopy on matrix-isolated samples at 29 K [15]. All of these workers are in agreement that the transition lies outside and at lower energy than the strong $\pi\pi^*$ absorption, and the clearly resolved excitation spectrum places E(0-0′) at 31.4×10^3 cm^{-1} (318 nm).

These experimental results for purine are summarized and compared with those for adenine and with the data from six semi-empirical MO calculations in table 2. Consideration is restricted to the lowest $n\pi^*$ and the two lower $\pi\pi^*$ transitions. The well-established $n\pi^*$ transition of purine is not satisfactorily accounted for by the sole published calculation (an all-valence electron CNDO-CI method), the calculated level actually lying above the lowest $\pi\pi^*$ transition [42]. The same behavior is found for adenine, the calculated $n\pi^*$ lying at 228 nm. When the result for purine is adjusted to agree with experiment, application to adenine of the 'corrective constant' ($\Delta E'$), thus derived still gives a value (253 nm) lying above the lowest $\pi\pi^*$ transition calculated to be at 258 nm. All other calculations, despite their range of absolute values, result in levels for $n\pi^*$ lying below the lowest $\pi\pi^*$ transition, in agreement with our experimental observations. The 'best' calculations (those producing values closest to those from experiments) seem to be those of the variable-electronegativity procedure of Srivastava and Mishra [46] and the preliminary results reported here using the HAM/3 method. Srivastava and Mishra actually find two low-lying $n\pi^*$ transitions with an energy separation of 2.8×10^3 cm^{-1}, and while it is tempting to correlate this with our two excitation spectra, also with an energy separation of 2.8×10^3 cm^{-1}, the present evidence is that our

Table 2

Experimental and theoretical transition energies for the lower states of purine and adenine (9-H)

		Experiment			Theory					
		293 K		20 K [c]	[42]	[43]	[44]	[45]	[46]	This work
Purine	$\pi\pi^*$	50 (200) [a]			41.8 (239)					
		38 (263)	37.9 [b]	37.1 (170)	38.7 (258)					
	$n\pi^*$	34 (294)	34.5 (290)	31.4 (318)	39.0 (256)					
Adenine (9-H)	$\pi\pi^*$	37.1 (270) [d]	39.2 (255) [e]	(77 K, this work)	40.7 (264)	40.9 (245)	41.0 (244)	39.1 (255)	37.1 (269)	37.9 (264)
		36.4 (275)	36.4 (275)	(this work)	38.7 (258)	40.0 (250)	40.25 (248)	37.5 (267)	35.6 (281)	36.7 (272)
	$n\pi^*$			33.0 (304)	43.8 (228)	38.2 (261)	38.8 (258)	36.0 (277)	35.3 (283)	34.5 (289)
				30.2 (331)					32.5 (308)	

[a] Ref. 44. [b] Ref. 42. [c] Refs. 15 and 16. [d] Ref. 7. [e] Ref. 2; all energies are expressed in cm$^{-1} \times 10^{-3}$ with the corresponding wavelength (in nm) in parentheses.

lowest energy excitation may be better described as an intermolecular charge transfer in the specific geometry of the adenosine crystal in which the NH_2 group of one adenosine molecule lies approximately above the midpoint of the C_4–C_5 bond of another: for this case, the calculation procedure of Srivastava and Mishra would be inappropriate. The HAM/3 method has been used successfully to correlate ionization energies in a photoelectron spectroscopic study of adenines [47]. The results are clearly sufficiently close to experiment to encourage further computations.

In retrospect, the reasons for the previous inability to detect the lowest $^1(n\pi^*)$ transition may be seen from the experimental and theoretical work reported here, namely, that the transition lies quite close to a (solvent-sensitive) $^1(\pi\pi^*)$ absorption and perhaps more importantly has an oscillator strength of approx. 5×10^{-4} (HAM/3) while purine is an order of magnitude stronger at 3.5×10^{-3} [39]. It is worth noting that a weak 'tail' absorption extending to 320 nm has been observed for sublimed films of adenine [48].

4.5. Impurity effects

In work such as that described here we have been concerned that we could be observing impurity effects, however, there are several reasons why we believe this is not a satisfactory explanation. First, the phosphorescence emission peaks clearly correlate with earlier observations from dilute organic glasses and the same emission is observed on excitation in the strong $\pi\pi^*$ band at 270 nm (fig. 3b). Unless the impurity by chance happens to have the same emission bands as adenosine, the possibility of emission by the impurity must be ruled out. Second, the change in emission spectra with excitation wavelength is not a shift in the emission wavelength. What does change is the distribution of intensities among the various vibronic peaks. This provides evidence for the existence of two emitting states (conformers perhaps?) of adenosine, and excitation transition B is not explicable as resulting from energy transfer from an absorbing impurity unless it selectively populates only one of the emitting states, a rather unlikely process for which we can see no rationalization. Third, the excitation spectrum for transition B has a vibronic splitting characteristic of the Raman spectrum of adenosine. Fourth, we have recently analyzed the adenosine for impurities by HPLC separation of an aqueous solution and only one elution peak was observed [49].

More complicated impurity models can be proposed, such as attributing excitation transitions A and B to two different impurities, only one of which by coincidence happens to be found in poly(rA) (normally expected to be less pure than adenosine). However, all explanations based on the presence of an impurity encounter the problem of selective population noted above.

Although none of these considerations is individually conclusive, collectively they constitute good reasons for regarding the observed behavior as being intrinsic rather than impurity-controlled. Further work is planned using single crystals and dilute organic glasses.

Acknowledgement

This work has been carried out with the support of PHS grant GM30474.

References

1 S.F. Mason, J. Chem. Soc. (1954) 2071.
2 R.F. Stewart and N. Davidson, J. Chem. Phys. 39 (1963) 255.
3 R.F. Stewart and L.H. Jensen, J. Chem. Phys. 40 (1964) 2071.
4 A.F. Fucaloro and L.S. Forster, J. Am. Chem. Soc. 93 (1971) 6443.
5 Y. Matsuoka and B. Norden, J. Phys. Chem. 86 (1982) 1378.
6 J. Ingwall, J. Am. Chem. Soc. 94 (1972) 5487.
7 D. Fornasiero, I.A.G. Roos, K.-A. Rye and T. Kurucsev, J. Am. Chem. Soc. 103 (1981) 1908.
8 M. Tsuboi, A. Hirakawa, Y. Nishimura and I. Hisada, J. Raman Spectrosc. 2 (1976) 609
9 D.C. Blazej and W.L. Peticolas, Proc. Natl. Acad. Sci, U.S.A. 74 (1977) 2639.
10 T.H. Bushaw, F.E. Lytle and R.S. Tobias, Appl. Spectrosc. 34 (1980) 521.
11 D.W. Miles, M.J. Robins, R.K. Robins and H. Eyring, Proc. Natl. Acad. Sci. U.S.A. 62 (1969) 22.
12 C.A. Bush, J. Am. Chem. Soc. 95 (1973) 214.

13 W. Voelter, R. Records, E. Bunneberg and C. Djerassi, J. Am. Chem. Soc. 90 (1968) 6163.
14 S.K. Lower and M.A. El-Sayed, Chem. Rev. 66 (1966) 199.
15 J.J. Smith, Photochem. Photobiol. 23 (1976) 365.
16 J.J. Smith, Spectrochim. Acta 32A (1977) 135.
17 V.G. Krishna and L. Goodman, J. Am. Chem. Soc. 83 (1961) 2042.
18 C. Helene, Physico-chemical properties of nucleic acids, ed. J. Duchesne (Academic Press, London, 1973) vol. 1, p. 119.
19 T.F. Lai and R.E. Marsh, Acta Crystallogr. B28 (1972) 1982.
20 C.E. Bugg, in: Proc. Fourth Jerusalem Symp. Purines: theory and experiment, ed. B. Pullman (Academic Press, New York, 1971) p. 178.
21 a.A. Rupprecht, Acta Chem. Scand. 20 (1966) 494.; b. A. Rupprecht, Biotechnol. Bioeng. 12 (1970) 93; c. A. Rupprecht, Acta Chem. Scand. B33 (1979) 779.
22 E. Lindholm and L. Åsbrink, Molecular orbitals and their energies studied by the semi-empirical HAM method. Lecture notes in chemistry (Springer-Verlag, Berlin, 1985) vol. 38.
23 M. Spencer, Acta Cystallogr. 12 (1969) 59.
24 E.P. Gibson and J.H. Turnbull, J. Photochem. 11 (1979) 313.
25 T. Nakota, M. Yamato, M. Tasumi and T. Miyazawa, Photochem. Photobiol. 22 (1975) 97.
26 J. Longworth, R.O. Rahn and R.G. Shulman, J. Chem. Phys. 45 (1966) 2930.
27 P. Szerenyi and H.H. Dearman, J. Chem. Phys. 58 (1973) 2467.
28 V. Kleinwächter, J. Drobnik and L. Augenstein, Photochem. Photobiol. 6 (1967) 133.
29 J. Drobnik, V. Kleinwächter and L. Augenstein, Photochem. Photobiol. 6 (1967) 147.
30 B.J. Cohen and L. Goodman, J. Am. Chem. Soc. 87 (1965) 5487.
31 R.C. Lord and G.J. Thomas, Spectrochim. Acta 23A (1967) 2551.
32 M. Tsuboi, S. Takahushi and I. Harada in: Physico-chemical properties of nucleic acids, ed. J. Duchesne (Academic Press, New York, 1973) vol. 2, p. 91.
33 T. Co and A.H. Maki, Biochemistry 17 (1978) 182.
34 F.H. Dörr and H. Gropper, Ber. Bunsenges. Phys. Chem. 67 (1963) 193.
35 M.A. El-Sayed and R.E. Brewer, J. Chem. Phys. 39 (1963) 1623.
36 T. Montenay-Garestier, C. Hélène and A.M. Michelson, Biochim. Biophys. Acta 182 (1969) 342.
37 V. Kleinwächter, J. Drobnik and L. Augenstein, Photochem. Photobiol. 7 (1968) 485.
38 M. Gueron, in: Basic principles in nucleic acid chemistry, ed. P.O.P. T'so (Academic Press, New York, 1974) vol. 1, ch. 4.
39 J. Drobnik and L. Augenstein, Photochem. Photobiol. 5 (1966) 13
40 M.J. Robey and I.G. Ross, Photochem Photobiol. 21 (1975) 363.
41 H.H. Chen and L.B. Clarke, J. Chem. Phys. 51 (1969) 1862.
42 W. Hug and I. Tinoco, J. Am. Chem. Soc. 96 (1974) 665.
43 N.V. Zheltovski and V.I. Danilov, Biofizika 19 (1976) 802.
44 F.A. Savin, Y.V. Morozov, A.V. Borodavkin, V.O. Chekhov, E.I. Budowsky and N.A. Simukova, Int. J. Quantum. Chem. 16 (1979) 825.
45 H. Ito and Y.J. I'Haya, Bull. Soc. Chem. Jap. 49 (1976) 3466.
46 S.K. Srivastava and P.C. Mishra, Int. J. Quantum Chem. 18 (1980) 827.
47 J. Lin, C. Yu, S. Peng, I. Akiyama, K. Li, L. K. Lee and P.R. LeBreton, J. Am. Chem. Soc. 102 (1980) 4627.
48 T. Yamada and H. Fukutome, Biopolymers. 6 (1968) 43.
49 J.-P. Ballini, M. Daniels and P. Vigny, Eur. J. Biophys. (1988) in the press.